Interaction with the Matrix: The Dominant Factor in Macromolecular Band Spreading in Gel Electrophoresis

Elena Yarmola,[†,‡] Peter P. Calabrese,[§] Andreas Chrambach,[†] and George H. Weiss*[,§]

Section on Macromolecular Analysis, Laboratory of Cellular and Molecular Biophysics, National Institutes of Health, Bethesda, Maryland 20892, Laboratory of Biopolymer Physics, Engelhardt Institute of Molecular Biology, Russian Academy of Sciences, Moscow, Russia, and Physical Sciences Laboratory, Division of Computer Research and Technology, National Institutes of Health, Bethesda, Maryland 20892

Received: September 19, 1996[⊗]

The conventional theory of electrophoretic processes is based on a model in which the migration process is determined by a biased diffusion process which predicts that the peak shape should be Gaussian. This implies that the peak position is proportional to time and the width (measured as the full width at half-maximum) is proportional to (time)$^{1/2}$. Recently developed instrumentation allows a more critical examination of both the assumptions and conclusions derivable from theory by intermittent scanning of the migration path. Data toward this end were collected on the kinetic behavior of phycoerythrin in an agarose gel. These data indicate significant deviations from a Gaussian shape and from results derivable from a model based on diffusion. A number of parameters that could be measured rather simply were compared with the predictions of both a diffusion-based theory and a non-Markovian theory, showing that the latter produced results in better accord with experiment. A practical implication of this finding is that the resolution of two peaks, after an initial transient period, need not increase with migration time.

I. Introduction

A standard assumption in quantitative interpretations of electrophoretic data obtained from a single pulse-loaded molecular species is that the variance associated with an isolated peak satisfies the relation $\sigma^2(t) = 2Dt$, where D is a diffusion constant. Approaches to the selection of a gel concentration for optimal species separation generally also implicitly involve an assumption of a Gaussian peak shape. The two assumptions, that of a linear dependence of $\sigma^2(t)$ on time and the Gaussian peak shape, are equivalent to saying that the concentration, $c(x,t)$, satisfies a diffusion equation with a field term having the form[1]

$$\frac{\partial c}{\partial t} = D\frac{\partial^2 c}{\partial x^2} - \mu E\frac{\partial c}{\partial x} \tag{1}$$

where μ is the mobility and E the field. The solution to this equation with the initial condition $c(x,0) = c_0\delta(x)$ is readily shown to be

$$c(x,t) = \frac{c_0}{\sqrt{4\pi Dt}}\exp\left(-\frac{(x-\mu Et)^2}{4Dt}\right) \tag{2}$$

The results of several recent studies appear to contradict both the basic assumptions and the results of the last paragraph. For example, the application of a gel electrophoresis device that allowed experimenters to intermittently scan the migration path of a DNA fragment of 1.8 kb length showed that the band of this species, initially electrophoresed into a 1% agarose gel, did not diffuse appreciably over a period of 30 h after the field was switched off.[2] Similarly, in some as yet unpublished experiments, N. Chen has shown that *R*-phycoerythrin (henceforth referred to as PHYCO), a native fluorescent protein of 290 kDa, does not diffuse noticeably over a period of hours in a 5% agarose gel; also PHYCO does not diffuse for 16 h in a capillary of 150 μm diameter containing un-cross-linked polyacrylamide solution.[3] Further, experiments suggest that the peak shape of PHYCO or fluorescein carboxylate-labeled conalbumin (CONALB-F) shows marked deviations from a Gaussian form, as a function of both migration time (or distance) and gel concentration.[4]

The question raised by these experimental findings is how to account for band spreading when diffusion is negligible in an electrophoresis system and when diffusion is negligible in the absence of a field. We will refer to such band spreading as "interactive dispersion" (hereafter, ID), since we propose that the mechanism of spreading is due to fluctuating interactions or entanglements of the protein with the gel matrix for random amounts of time during the course of its motion through the gel. Notice that peaks that spread by the ID mechanism can be Gaussian in appropriate circumstances, although the peaks observed in our experiments with PHYCO show an unmistakable degree of asymmetry around the peak maximum.

A recent study[5] has qualitatively distinguished ID from diffusional spreading in DNA fragments of 1, 2, and 3 kb lengths. Results of this study indicate that while both ID and diffusive spreading occur simultaneously during gel electrophoresis, ID becomes the predominant source of band spreading as the particle size increases. In the data reported in the present paper, the ratio $\sigma(t)/t$ is found to tend toward a constant value which contradicts the behavior $\sigma^2(t) = 2Dt$ that follows as a consequence of eq 2.

An alternative phenomenological two-state model of the electrophoretic (as well as a more general chromatographic) process has been suggested to account for these findings.[4] This model, originally formulated by Giddings and Eyring[6] in a simplified form, was generalized later to include more complicated non-Markovian effects.[7] The basic idea in the theory is that protein motion through the gel can be represented as a succession of times during which the motion is unimpeded, interrupted by periods during which it is immobilized due to

[†] Section on Macromolecular Analysis.
[‡] Laboratory of Biopolymer Physics.
[§] Physical Sciences Laboratory.
[⊗] Abstract published in *Advance ACS Abstracts,* March 1, 1997.

S1089-5647(96)02893-3

entanglement with the gel. Both types of time are random variables. When these variables are "fractal times" as defined by Shlesinger,[8] the peaks can indeed be asymmetric as follows from the analysis in ref 7.

In this paper we compare four easily measured parameters that characterize electrophoretic peaks, showing that they are at least qualitatively similar to predictions of the non-Markovian theory. These are the position of the peak, the peak amplitude, the full width at half-maximum of the peak, and the degree of peak asymmetry, all considered as functions of time. A more detailed comparison of theoretical and experimental peak shapes will be left for later, since these require considerably more numerical analysis.

II. Materials and Methods

Our experiments were all carried out on PHYCO, which is a sufficiently large protein that ordinary diffusion can be neglected as the principal source of peak spreading. The use of PHYCO is advantageous because the sole commercially available instrument for real-time peak scanning in electrophoresis, the HPGE-1000 instrument, is only designed for detecting fluorescence. PHYCO is nearly unique among proteins in that the fluorescent group is part of the native molecule. This avoids artifacts due to fluorescing groups that remain adsorbed noncovalently after gel filtration whenever a nonfluorescing protein is labeled with a fluorogenic agent. A protein, rather than, say, a DNA fragment, was chosen for the investigation since protein shape is not significantly altered as it moves through a gel. In contrast, DNA tends to be stretched as it passes through a gel.

The gel medium in our set of experiments was Agarose SeaPrep 15/45. This was chosen since, due to a 10% derivatization with hydroxymethyl groups, it is the most soluble of commercially available agaroses. It can therefore be prepared at high enough concentrations to provide a gel with a pore size appropriate for use with proteins. Its retardation coefficient has been shown to be such that dK_R/dR approximates that of polyacrylamide gels.[9]

The protein PHYCO was obtained from Polysciences (Warrington, PA, cat. no. 18188), and the SeaPrep agarose was obtained from FMC, Rockland, ME (cat. no. 50302). The buffer 0.015 M Tricine (Calbiochem cat. no. 39468) and 0.015 M Tris, pH 8.17, was used as a continuous buffer in all phases. The gel buffer contained 1% glycerol.

The experiment was performed using an automated commercial gel electrophoresis instrument (HPGE-1000, LabIntelligence, Belmont, CA) using agarose (2−4%) gels. The agarose solution in gel buffer (140 mL) was weighed, heated to boiling in a microwave oven, and stirred at 1 min intervals until it dissolved. The hot solution was weighed, hot water was added to the original weight, and the solution was cooled to about 50 °C with magnetic stirring. The legs of the gel tray were sealed with Parafilm, and the solution was pipetted to the height of the partitions of the gel tray containing the Teflon slot former described in ref 10. It was then cooled for about a half hour at room temperature and subsequently for 1 h at 4 °C. At this point the tray was inserted into the electrophoretic apparatus which was set to maintain a temperature of 5 °C, and the sample was applied 27 mm from the cathodic end of the gel. The field strength was kept constant at values of 2.5−40 V/cm in different experiments. Scans were made at regular intervals which ranged from 5 to 30 min during the electrophoretic phase and from 30 to 90 min when assaying diffusive properties.

III. Theoretical Background

As mentioned, our analysis is based on a model consisting of two states, the mobile state (M) and the immobilized state

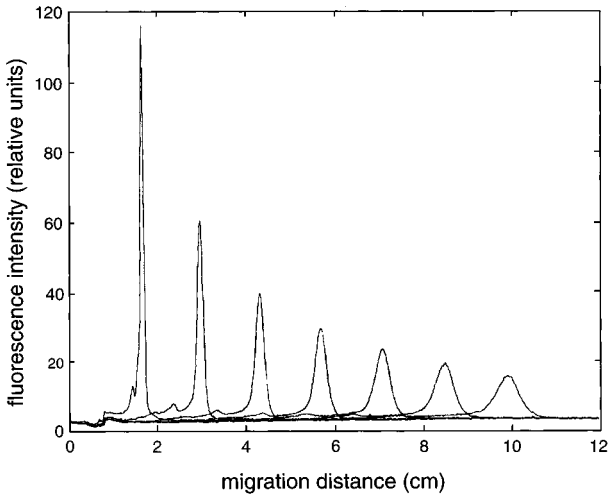

Figure 1. Representative peak shapes of protein bands as determined by the HPGE-1000 instrument based on intermediate scanning of fluorescence. Representative peaks generated by phycoerythrin in agarose gel electrophoresis (3% SeaPrep, 0.015 M Tris−tricinate; pH 8.2, 1% glycerol, 5 °C, 20 V/cm).

(I). During migration through the gel, a given molecule makes many interchanges between the two states. The rules that determine the kinetics are (1) the transition M → I is assumed to be first order with rate k, and (2) the time spent by a single protein in the entangled state is a random variable whose properties are described by a probability density $\psi(t)$. In this picture the choice $\psi(t) = k' \exp(-k't)$ is equivalent to the statement that I → M likewise follows first-order kinetics. However, we will want to consider more general choices of the function $\psi(t)$.

If the diffusion constant is set equal to 0, consistent with experimental findings with the PHYCO molecules, then it is shown that the concentration $c(x,t)$ satisfies an equation of the form

$$\frac{\partial c(x,t)}{\partial t} = -v\int_0^t Q(t-\tau)\frac{\partial c(x,\tau)}{\partial x}\,d\tau \qquad (3)$$

where v is the velocity ($v = \mu E$) that is obtained in the absence of entanglements and $Q(t)$ is a function defined in terms of k and $\psi(t)$. Motion at the constant speed v corresponds to the choice $Q(t) = \delta(t)$. When motion is impeded due to entanglement with the gel only, an expression for the Laplace transform $\hat{Q}(s) = \int_0^\infty Q(t)\exp(-st)\,dt$ is known. The relation of $\hat{Q}(s)$ to the transform $\hat{\psi}(s)$ is found to be

$$\hat{Q}(s) = \left[1 + \frac{k\{1-\hat{\psi}(s)\}}{s}\right]^{-1} \qquad (4)$$

and the solution to the Laplace transform of eq 3 with the initial condition $c(x,0) = \delta(x)$, which corresponds to pulse loading $c(x,0) = c_0\delta(x)$, is[7]

$$\hat{c}(x,s) = \frac{c_0}{v\hat{Q}(s)}\exp\left[-\frac{sx}{v\hat{Q}(s)}\right] \qquad (5)$$

We remark, parenthetically, that it is also possible to include a diffusion term in eq 3 but its effects can be shown to be secondary to those due to the convection term in that equation when the second moment of $\psi(t)$ is infinite. Notice that even without an explicit diffusive term there is still a mechanism for peak spreading included in the simpler version of our model

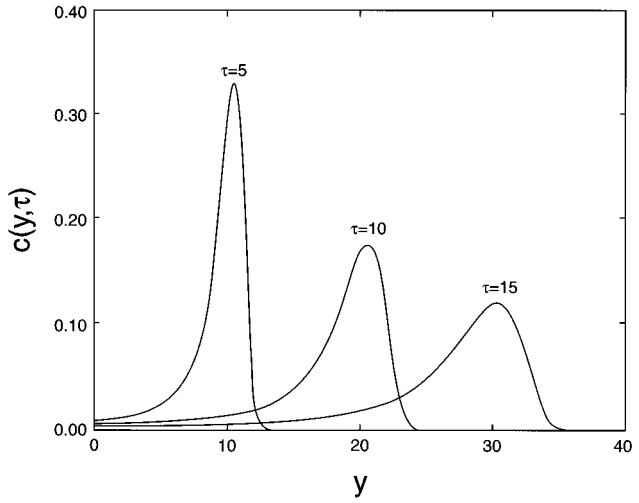

Figure 2. Typical profiles generated by numerically inverting eq 11 with $\beta = 0.1$ for the values of $\tau = 5$, 10, and 15. $c(y,\tau)$ is the concentration in terms of the dimensionless variables y and τ. The peaks show the same qualitative behavior as the experimental ones shown in Figure 1.

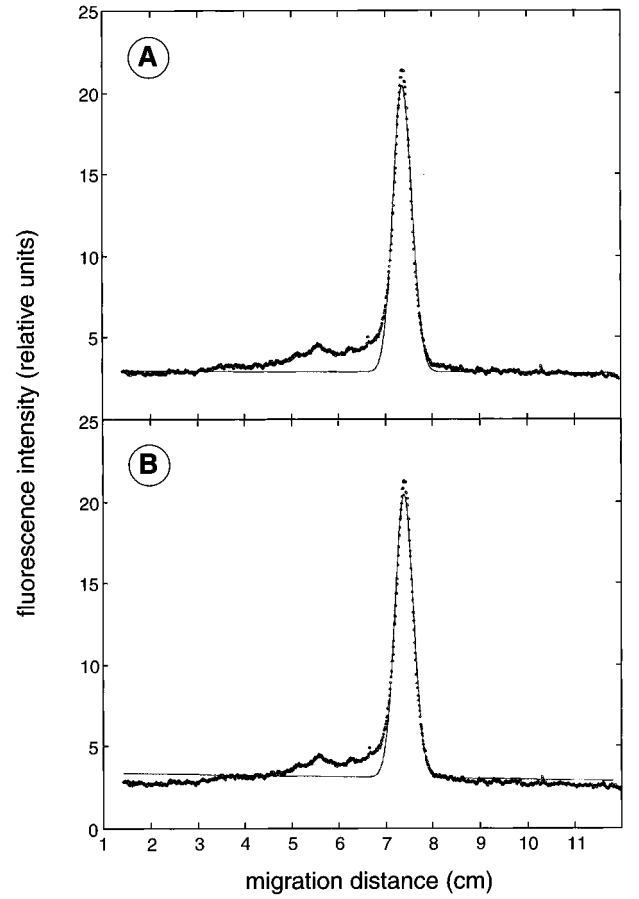

Figure 3. (A) A typical peak with the base line selected by a "best" fit to the longitudinal extension of both sides of the peak (tails). (B) The same data but with the base line selected by fitting the data to the sum of a Gaussian profile and a line with a possibly nonzero slope. The fit was made using the MATLAB program.

(provided that $\hat{Q}(s)$ is not a delta function, as remarked above) which is a consequence of fluctuations in the entanglement times.

The analysis to this point is exact, within the purview of the model. To make contact with our experimental data we make the further assumption that $\psi(t)$ has a specific behavior at long times, which is to say that

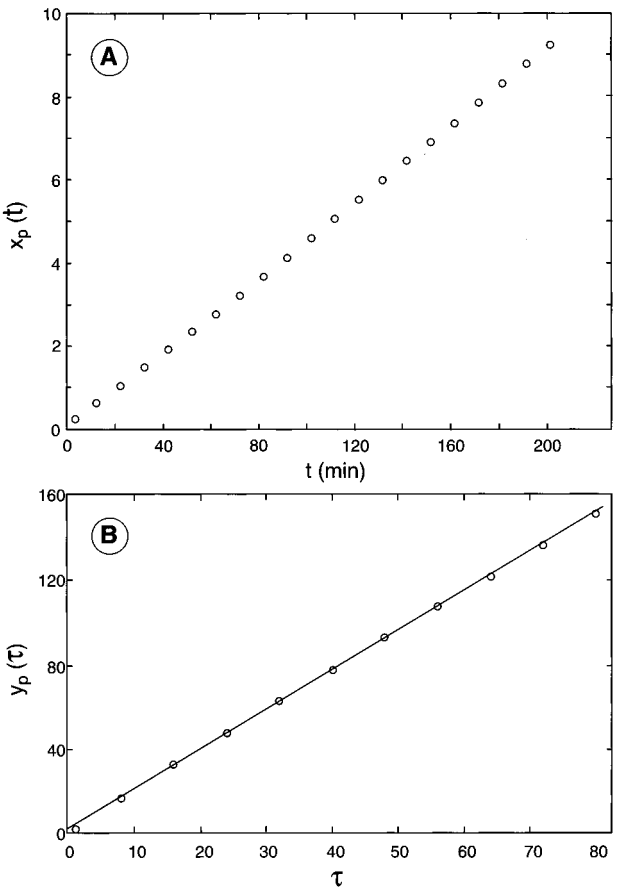

Figure 4. (A) A plot of the migration distance of the peak maximum $x_p(t)$ as a function of time for the experimental system with properties described in the caption of Figure 1. The circles are the data, and the line is the best fit to the data. It is evident that $x_p(t)$ is very close to being a linear function of t. (B) A plot of $y_p(\tau)$, the migration distance of the peak maximum in dimensionless units, generated from eq 11 with $\beta = 0.1$.

$$\psi(t) \cong \frac{T^{\alpha}}{t^{\alpha+1}}, \quad t \gg T \tag{6}$$

where T is a constant time. The exponent α is chosen to satisfy $1 < \alpha \leq 2$ which means that a single sojourn in the entangled state has a finite first moment but the associated variance is infinite. Call the first moment μ, i.e., the average residence time in a single sojourn in state I is equal to μ. When the property specified in eq 6 holds, the transform $\hat{\psi}(s)$ can be expanded[11] around $s = 0$ as $\hat{\psi}(s) \approx 1 - s\mu + (sT)^{\alpha}$ which suffices to determine physical properties at times after which the number of interchanges between I and M are large. The stated expansion is equivalent to the statement that $\hat{Q}(s)$ can be expanded around $s = 0$ as

$$\hat{Q}(s) \approx Q_0 + Q_1 s^{\alpha-1} = Q_0 + Q_1 s^{\beta} \tag{7}$$

where $\beta = \alpha - 1$ is between 0 and 1. This follows by substituting the small-s expansion of $\hat{\psi}(s)$ into eq 4. The parameters Q_0 and Q_1 that appear in eq 7 are

$$Q_0 = (1 + k\mu)^{-1}, \quad Q_1 = Q_0^2 k T^{\alpha} \tag{8}$$

After substituting eq 7 into eq 5, that equation can be written in terms of dimensionless units, greatly diminishing the amount of numerical inversion of Laplace transforms required for our purposes. The transformation is effected by defining a dimensionless time τ and a dimensionless distance y by

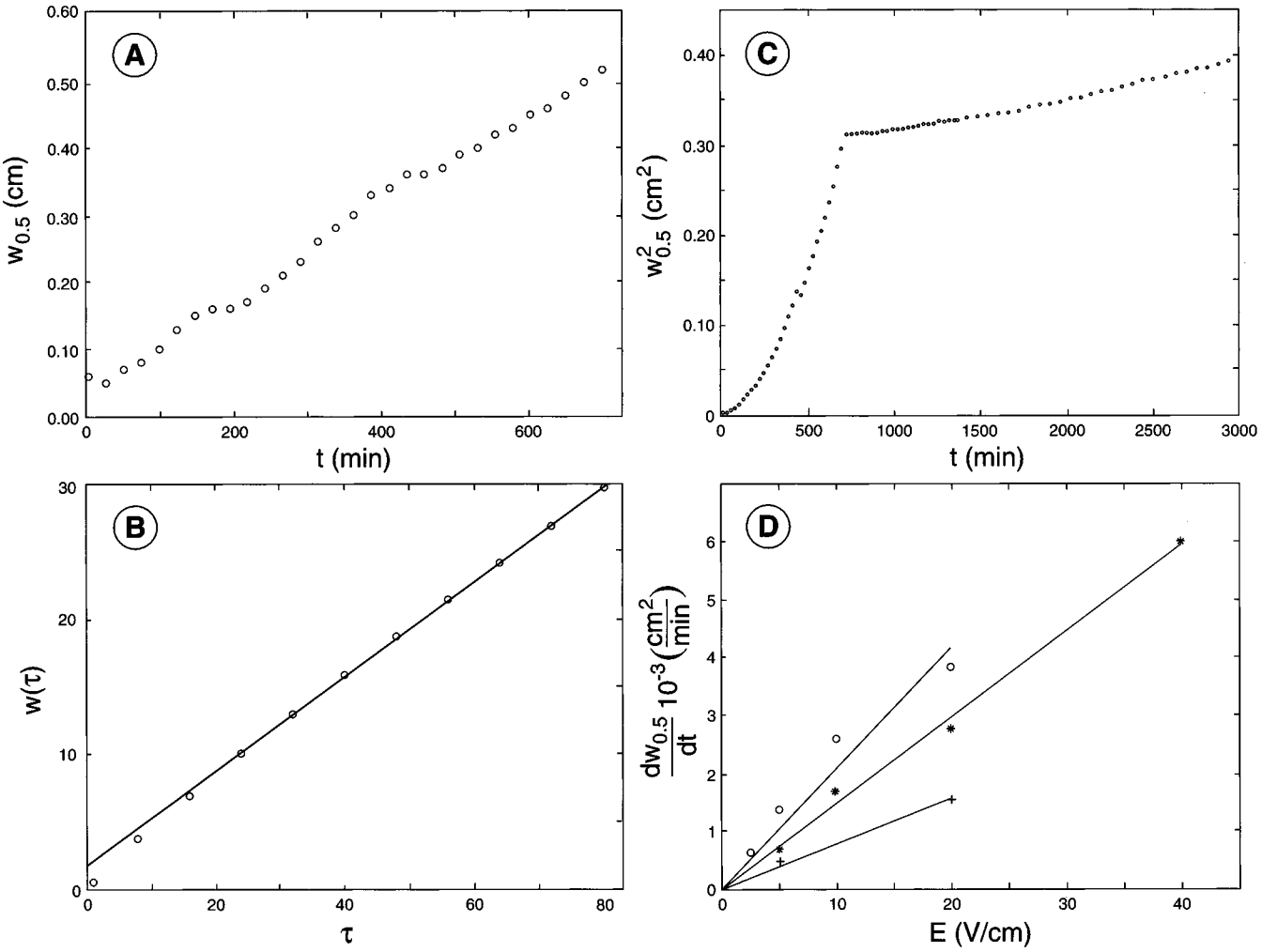

Figure 5. (A) A plot of the fwhm $w_{0.5}(t)$ derived from the system whose parameters are given in the caption to Figure 1 except that the field strength was 5 V/cm. The data are approximately linear in t, which is to be contrasted to proportionality with $t^{1/2}$ as predicted by a diffusion-based model. (B) A plot of the dimensionless $w_{0.5}(\tau)$ calculated from the numerical inverse of the transform in eq 11 with $\beta = 0.1$. Except at the smallest values of τ, the width is seen to increase linearly with time. (C) $w^2_{0.5}(t)$ obtained for an experiment in which a field was applied for 720 min and then switched off. During the field-on period, $w^2_{0.5}(t)$ is clearly not a linear function of time, and in the field-off period it is, albeit with a very small slope consistent with diffusion. Because the slope is so small we have set the diffusion constant equal to zero in the text to simplify the analysis. (D) A plot of the derivative $dw_{0.5}(t)/dt$ as a function of the field strength at different gel concentrations indicating a linear dependence of the slope. The circles correspond to a gel concentration of 2%, the stars to 3%, and the crosses to 4%.

$$\tau = t/\mathcal{T},\quad y = x/(Q_0 v \mathcal{T}) \tag{9}$$

where

$$\mathcal{T} = \left(\frac{kT^{\beta+1}}{Q_0}\right)^{1/\beta} \tag{10}$$

This sequence of substitutions transforms eq 5 to

$$\hat{\mathbf{c}}(y,\sigma) = \frac{c_0}{vQ_0\mathcal{T}(1+\sigma^\beta)} \exp\left[-\frac{y\sigma}{1+\sigma^\beta}\right] \tag{11}$$

in which σ is the transform variable associated with τ. Thus, for a given value of β and y, just a single numerical Laplace inversion need be performed after which only simple changes of variables allow scanning the effects of changes in all of the remaining constants. Notice that eq 11 is normalized in the sense that $\int_{-\infty}^{\infty} c(y,\tau)\, dy = c_0(vQ_0\mathcal{T})^{-1}$ which is equivalent to normalizing $c(x,t)$ to the initial concentration c_0.

Although the assumptions in eqs 6 and 7 are somewhat arbitrary, they do provide results that are at least in qualitative agreement with the experimental data shown in Figure 1. This is demonstrated by some curves generated by numerically inverting eq 11 using the algorithms suggested by Dubner and Abate[12] and as modified by Crump.[13] The results of these inversions are shown in Figure 2 for $\beta = 0.1$.

IV. Details of the Data

Before presenting comparisons between theoretical predictions and experimental data, we mention some further details related to our examination of the experimental results. An occasionally vexing difficulty in electrophoretic experiments is that of properly identifying a base line. As exemplified by the data plotted in Figure 3, we used two techniques to identify the base line. The first of these was to find the best linear fit to the horizontal stretches of the data, i.e., of measured data away from the immediate vicinity of the peak. The second was to approximate the peak by a Gaussian, which should yield a good fit in the immediate vicinity of the peak maximum, and find the best fit to the sum of the Gaussian peak and a linear function. A comparison of the results showed little difference between the base line obtained by the two techniques, as illustrated by examining Figure 3.

A glance at Figure 1 indicates that the PHYCO preparation is not entirely homogeneous, there being a small bump on the

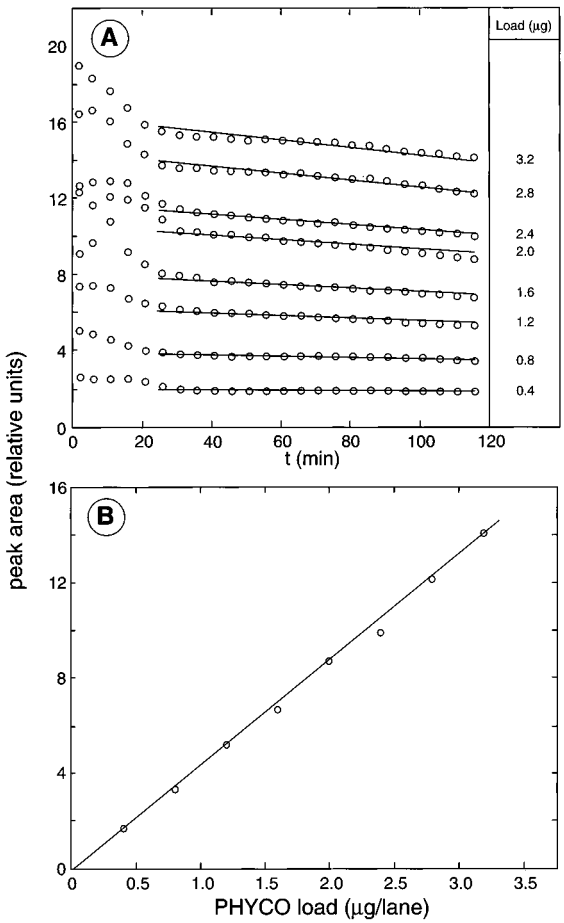

Figure 6. (A) The slow decrease of the peak area as a function of migration time. The lines represent fits of the data to a first-order disappearance rate after data obtained during a short transient time period were eliminated. Each of the lines could be fit by $c(t) = c(0)\exp(-kt)$, where t is the time in minutes and $k = 0.0015$ min^{-1}. The experimental conditions are those described in the caption to Figure 1 with a 2% agarose concentration. The numbers on the right-hand side correspond to different initial loads (μg/lane). (B) Peak area as a function of initial PHYCO load, showing the expected linear increase. The tails of the peaks were neglected in calculating the peak area.

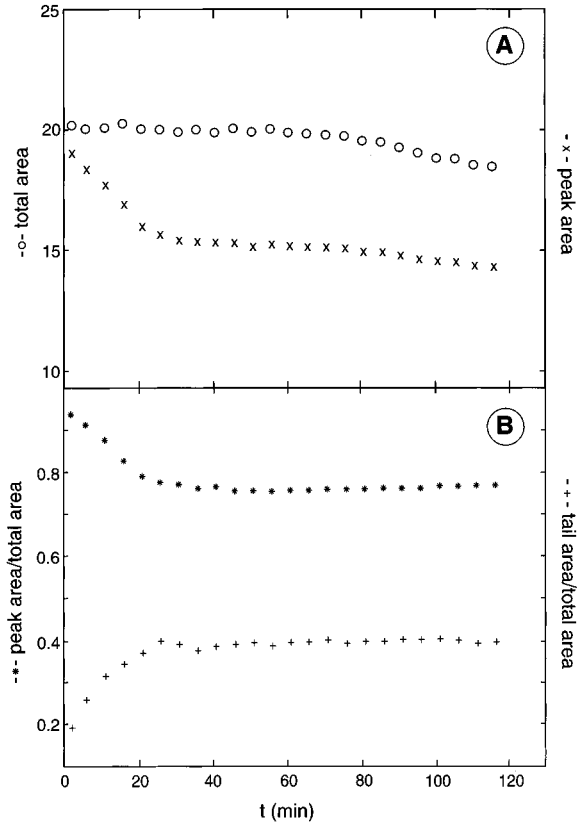

Figure 7. (A) Dependence of relevant areas on time. The circles represent the total scan area above the base line, while the stars represent the peak area as determined by truncating the concentration profile at a distance equal to 3σ, where σ is determined by the best Gaussian fit in the neighborhood of the peak maximum. After an initial transient, both areas appear to flatten out and remain constant as a function of time. (B) A similar plot comparing the variation of the ratio of peak area to total area as defined in Figure 7A and the tail areas as defined by truncating the peak at $w_{0.5}(t)$.

trailing edge of the peak. We attribute this to contaminant since its separation from the main PHYCO peak increases with increasing gel concentration.[15] Once separated, the auxiliary peak does not form anew under our experimental conditions. Examination of this contaminant by a Ferguson plot analysis indicates that it is not an oligomer of phycoerythrin. The contaminant is larger than the main PHYCO component since its separation is improved by increasing the gel concentration.[15]

V. Results

A. Time Dependence of the Peak Position. The first parameter to be examined is the position of the peak as a function of time, $x_p(t)$. Figure 4A suggests that in experimentally obtained data the peak position $x_p(t)$ is linear in time. Numerical calculations based on the model in eq 3, or equivalently in eq 5, also predict that at sufficiently long times $y_p(\tau)$ is essentially linear in time, which agrees with the experiments as illustrated in Figure 4B.

B. Time Dependence of the Full Width at Half-Maximum (fwhm). When the electrophoretic process is modeled as a diffusion process as in eq 2, the width at half-height $w_{0.5}(t)$ of a peak will be proportional to $t^{1/2}$. Figure 5A shows that a closer fit to the present data is obtained by assuming that $w_{0.5}(t)$ is proportional to t. This is a first indication that diffusion theory does not provide a model adequate for the analysis of the present set of data. This linear dependence on time was found to hold for loads in the range 0.2−3.2 μg/lane (data not shown) and did not appear to depend on the load at the field strengths and gel concentrations used in this study. This linear dependence agrees with the theoretical prediction obtained from a numerical inversion of the transform in eq 11 as seen in Figure 5B. Figure 5C contrasts the time-dependent behavior of (fwhm)^2 both in response to an applied field and in the absence of an electric field in which case only diffusion should be operative. In the former case, the behavior of (fwhm)^2 is a nonlinear function of the time, while in the latter case (fwhm)$^2/t$ is constant, as is evident from the data shown in the figure. The data in Figure 5D suggest that $dw_{0.5}(t)/dt$ varies approximately linearly with the applied electric field, in agreement with the corresponding predictions of our model.

C. Time Dependence of the Peak Area. To a reasonable approximation, the peak area remains constant at the lowest loads (Figure 6A) as implied by the theory. At higher loads the areas decrease slightly with time. Figure 6B confirms that the peak area is proportional to the load, as should be the case. The different areas to be discussed were all found to be proportional to the load, as one might expect. So far, unpublished data[15] show that the decrease cannot be attributed to progressive adsorption to the gel but is likely to be due to some form of photochemical damage to the fluorescent group which increases with load at early migration times.

To make our next point, we define what will be referred to as the dominant peak by finding a best Gaussian approximation

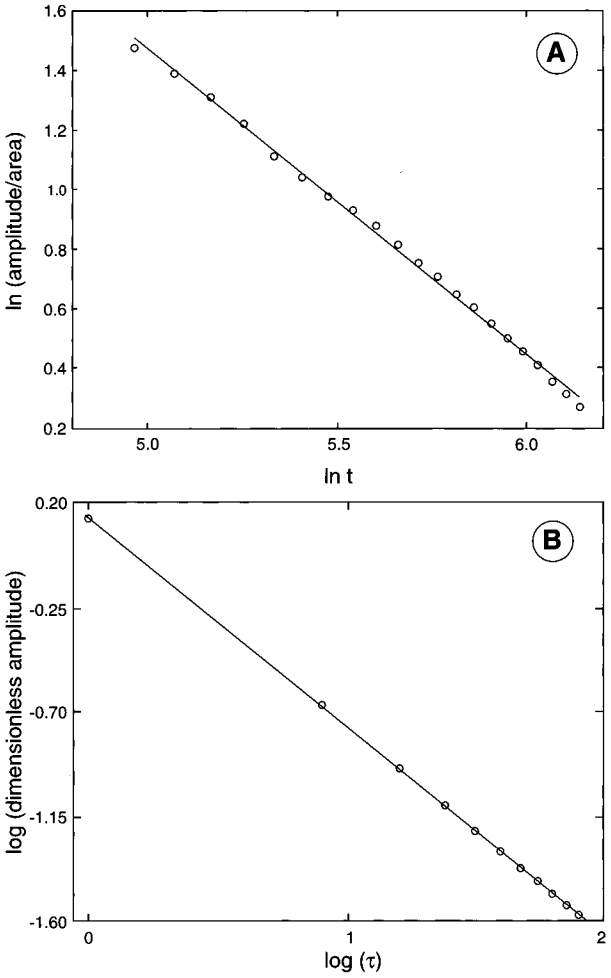

Figure 8. (A) ln[peak height/area] as a function of the time *t*. Data points (open circles) and the best fit straight line are shown. The equation of the fitted line is ln[peak height/area = 6.63 − 1.03 log *t*. (B) An equivalent curve generated by the numerical inversion of eq 11 with $\beta = 0.1$. The slope of this straight line was found to be −0.91.

to the center of the peak. This includes all of the concentration profile out to a distance 3σ (where σ is calculated from the best Gaussian fit to the peak) to either side of the peak position. The data in Figure 1 suggest that the phycoerythrin preparation is not entirely homogeneous. This inhomogeneity shows up as tailing in the ascending limb of the concentration profile. The parallelism between the two curves in Figure 7A indicates that tailing is not generated outside of a short initial period. This is also implied by the data shown in Figure 7B.

D. Time Dependence of the Peak Height. The pure diffusion model in eq 1 predicts that the peak height should decrease as $t^{-1/2}$. This was not found to be the case in our data. Figure 8A plots ln[peak height/area] as a function of ln *t*. In contrast to what might be expected from diffusion theory, the slope of the line in this plot was found to be −1.03. A similar exponent is found in numerical calculations not reported here. While we have not scanned the entire range in β to find a best fit to the experimental data, the curve in Figure 8B was plotted from data generated for $\beta = 0.1$ and gives a slope approximately equal to −0.9. Notice that the fact that the width times the height is approximately equal to 1 is consistent with the constancy of peak area as a function of time.

E. Time Dependence of Peak Asymmetry. Figure 9A defines the partial widths at the half-maximum of the peak, $w_+(t)$ and $w_-(t)$. A measure of the degree of asymmetry in the peak is the parameter

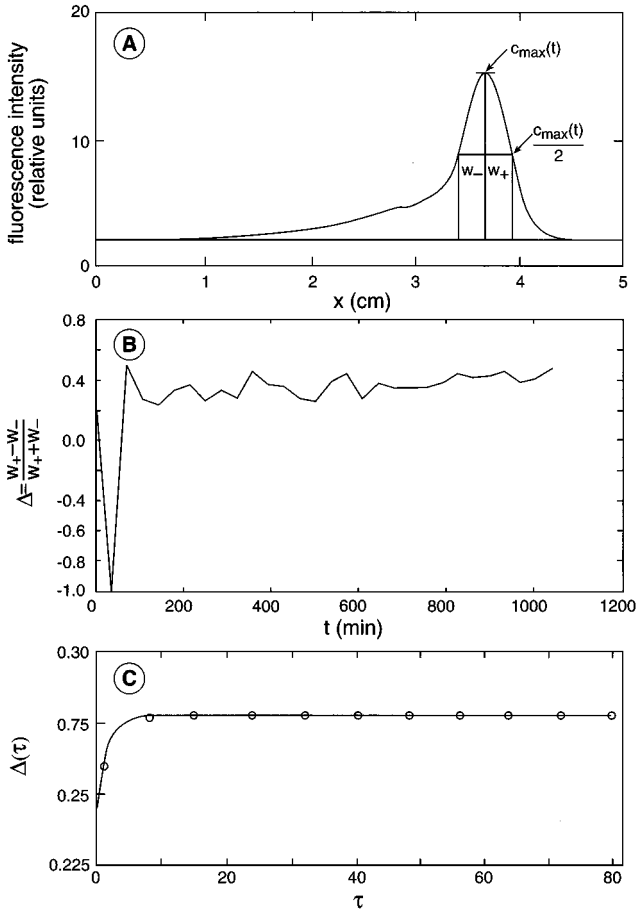

Figure 9. (A) Definition of the partial widths at half-height w_+ and w_- of a peak. (B) Typical curve of Δ plotted as a function of migration time, *t*. The parameters used in the experiment were those of Figure 1 except that the agarose concentration was 4% and the field strength 5 V/cm. (C) $\Delta(\tau)$ as generated from eq 11 with $\beta = 0.1$.

$$\Delta(t) = \frac{w_+(t) - w_-(t)}{w_+(t) + w_-(t)} \tag{12}$$

Diffusion theory implies the result $\Delta(t) = 0$ for all values of *t*. Some of our experimental data are plotted as a function of time in Figure 9B, and comparable results generated from the model in eq 11 are shown in Figure 9C. In both cases the tendency is for $\Delta(t)$ to approach a nonzero constant value after a short initial period.

VI. Discussion

We have seen that the model whose principal result is found in eq 11 is capable of reproducing at least several of the qualitative properties observed in our data which are otherwise incompatible with a diffusion-based model. While our specific version of the non-Markovian model should be used with caution at the present time because of a lack of more detailed comparisons with experimental data, the results of the present investigation suggest that fluctuations in the entanglement time with the gel fibers mainly determine the observed dispersion in the electrophoretic process. The standard diffusion constant is temperature-dependent and independent of the electrical field strength at low voltages, while the mechanism of ID is presumably independent of temperature but dependent on the voltage. This might occur because an increase in voltage tends to increase the number of contacts between the protein and the gel fibers.

Resolution is the central concern of separation science in general, and gel electrophoresis in particular. The lack of

apparent resolution at very low migration distances is generally thought to reflect a failure to detect small differences in peak positions, widths, and gaps between peaks. Our data could be fit by the functional form $w_{0.5}(t) = w_0 + at$ where w_0 and a are constants. This experimental finding that peak width in gel electrophoresis can be proportional to t rather than $t^{1/2}$ suggests reconsideration of the standard definition of a parameter, $R(t)$, that is used to measure resolution in chromatographic processes. This parameter that measures the extent of separation of two proteins combines the peak positions $x_i(t)$, $i = 1$ or 2, and the variances $\sigma_i^2(t)$ into the formula[1]

$$R(t) = \frac{x_1(t) - x_2(t)}{\sigma_1(t) + \sigma_2(t)} \tag{13}$$

In models based on Gaussian peak shapes, the $\sigma_i(t)$ are proportional to peak widths, so that if $c(x,t)$ satisfies the diffusion equation in eq 1, $R(t)$ is proportional to $t^{1/2}$. This implies that any degree of resolution is attainable provided that the experiment is run for a long enough period of time. In contrast, our data for PHYCO in an agarose gel indicate that $R(t)$ approaches a constant value with increasing time. This agrees with widespread experimental experience that increasing migration time does not increase resolution. It would clearly be desirable to extend this study to other proteins to determine the universality of the present results.

We have not, as yet, examined the consequences of our experimental results on other measures of resolution, such as one recently suggested and analyzed by Aldroubi and Garner.[14] The investigation reported on here relates only to gel electrophoresis. We plan to conduct a similar study of peak shape in capillary zone electrophoresis to see whether significant differences emerge in that type of experiment.

Finally, we comment that the experimental investigation reported on here was conducted on a highly soluble agarose rather than on polyacrylamide which is the conventional gel matrix for protein separations. This is justified by a comparative study of protein resolution in a variety of gel media[16] which showed that the selected agarose type, SeaPrep 15/45, is the matrix with the highest resolving power for native proteins, surpassing that of polyacrylamide.

References and Notes

(1) Giddings, J. C. *Unified Separation Science*; Wiley-Interscience: New York, 1991.
(2) Yarmola, E.; Chrambach, A. *Electrophoresis* **1995**, *16*, 345.
(3) Radko, S. P.; Chrambach, A. *Appl. Theor. Electrophor.* **1995**, *5*, 79.
(4) Weiss, G. H.; Sokoloff, H.; Zakharov, S. F.; Chrambach, A. *Electrophoresis* **1996**, *17*, 1325.
(5) Yarmola, E.; Sokoloff, H.; Chrambach, A. *Electrophoresis* **1996**, *17*, 1416.
(6) Giddings, J. C.; Eyring, H. *J. Phys. Chem.* **1955**, *59*, 416.
(7) Weiss, G. H. In *Transport and Relaxation in Random Materials*; Klafter, J., Rubin, R. J., Shlesinger, M. F., Eds.; World Scientific: Singapore, 1985; p 394.
(8) Shlesinger, M. F. *Annu. Rev. Phys. Chem.* **1988**, *39*, 269.
(9) Buzas, Z.; Chrambach, A. *Electrophoresis* **1982**, *3*, 121.
(10) Yarmola, E.; Chrambach, A. *Electrophoresis* **1995**, *16*, 350.
(11) Weiss, G. H. *Aspects and Applications of the Random Walk*; North-Holland: Amsterdam, The Netherlands, 1994; Chapter 5.
(12) Dubner, H.; Abate, J. *J. Assoc. Comput. Mach.* **1968**, *15*, 115.
(13) Crump, K. S. *J. Assoc. Comput. Mach.* **1976**, *23*, 89.
(14) Aldroubi, A.; Garner, M. M. *BioTechniques* **1992**, *13*, 620.
(15) Zakharov, S. F.; Kwok, S. H.; Sokoloff, H.; Chang, H.-T.; Radko, S. P.; Chrambach, A. *Appl. Theor. Electrophor.* **1997**, in press.
(16) Chen, N.; Chrambach, A. *Electrophoresis* **1997**, in press.